FLARES ON THE SUN : SELECTED RESULTS FROM HINOTORI

Katsuo Tanaka

Tokyo Astronomical Observatory, University of Tokyo
Mitaka, Tokyo, Japan

ABSTRACT
     The X-ray observations of solar flares by Japanese astronomy
satellite Hinotori (ASTRO-A) are reviewed. Detailed results from the X-
ray telescope and the soft X-ray spectrometers are given. The hard X-
ray images in the 17-40 keV range show a wide variety of source structures.
Examples of compact single source, stationary coronal source, and double
sources are presented. High resolution spectra in the range 1.7-2.0A
indicate strong turbulence and blue-shifted components in the beginning
of flares. From the FeXXV and FeXXVI spectra two kinds of thermal
plasma are shown to appear. The cooler component of $Te=15-20x10^6$K,
which increases in the impulsive phase of the hard X-ray burst, is
suggested to be produced by the dissipation of the electron beams. The
hotter component of $Te=30-50x10^6$K and $Ne=10^{11}-10^{12}$ cm^{-3} increases towards
the flare maximum. This component is also responsible for emitting 17-
40keV continuum, and emitted from a very compact source. The results
are discussed in comparison with flare loop models. It is shown that
evolutionary changes in the loop density realize various source structures
in the hard X-ray under the unitary electron beam hypothesis.

1. INTRODUCTION OF HINOTORI SATELLITE

     A Japanese astronomy satellite ASTRO-A was launched on February 21,
1981, from Kagoshima Space Station (KSC) by the Institute of Space and
Astronautical Science (ISAS). This satellite, nicknamed Hinotori
(Japanese for Fire Bird), is intended to observe various aspects of
solar flare X-rays with good spatial, spectral and temporal resolutions.
The physical instruments aboard Hinotori for flare studies are (1) Solar
X-ray Telescope (SXT) with Solar X-ray Aspect Sensor (SXA), (2) Soft X-
ray Crystal Spectrometer (SOX), (3) Soft X-ray Flare Monitor (FLM), (4)
Hard X-ray Flare Monitor (HXM) and (5) Solar Gamma Ray Detector (SGR).
Table summarizes these instruments.

Table Characteristics of Hinotori Instruments for Flare Observations

	Detector	Energy Range	Resolutions
SXT	113cm^2 NaI Scint.	17-60keV/5-10kev	38"(7")/~8sec ⎫
	113cm^2 NaI Scint.	17-60keV/5-10keV	30"(7")/~8sec ⎬(~4sec)
SXA	Fine Solar Aspect Sensor		5"
HXM	57cm^2 NaI Scint.	17-40keV	7.8ms (HXN-1)
		40-340keV	125ms (HXM-2-7)
SGR	62cm^2 CsI Scint.	210-6700keV	128channels/2sec
FLM	0.5cm^2 Xe Gas	2-25keV	128channels/4sec
	Scint.Prop.	counts in L/H bands	125ms
SOX	SiO2/NaI Scint.	1.72-1.95A	2mA/8sec
	SiO2/NaI Scint.	1.83-1.89A	0.15mA/8sec

Hinotori is a spinning satellite (about 4rpm) with its spin axis being off-set from the Sun center by 1.2°±0.5°. X-ray image and line spectrum are obtained utilizing this attitude and spin. The data processor aboard Hinotori judges a flare automatically and about 20 minutes data of a flare, preferentially for large flare, are stored in the data recorder. Real time data and recorded data are transmitted at KSC in about 12 minutes for each of five visible orbits per day. In a year and five months operation Hinotori observed 675 flares including 31 X-class flares. The largest flare was a X12 flare that occurred at 16:30UT of June 6, 1982. Early results have appeard in the proceedings of Hinotori Symposium (1982 January at ISAS). Here I review some selected results from this symposium as well as other preliminary results obtained by now.

2. RESULTS FROM THE SOLAR X-RAY TELESCOPE

Solar X-ray Telescope (SXT) is a rotational modulation collimator ("Oda" collimator) consisting of two orthogonal bigrid collimators and NaI scintillation counters. Flare position is determined in terms of optical lenses and collimators system (SXA) co-aligned with the X-ray collimators. Informations necessary to reconstruct the X-ray image from modulation patterns are obtained every quarter of the spin period or about 4s. For the image reconstrucion two kinds of methods : arithmetric reconstruction technique (ART) and maximum entropy method (MEM) have been used. Spatial resolution is determined nominally by FWHM of the triangular beam pattern (about 30"). However, due to the sharpness of the pattern edge SXT has a response to a structure less than 7" (Makishima 1982 HS-abbreviation for the proceedings of Hinotori Symposium). For a year after the launch the two collimators were mainly used for the hard X-ray range (17-40keV) with one collimator being switched to soft X-ray range (5-10keV) only for the later phase of flares.

General survey of some dozen flares performed by S. Tsuneta, T. Takakura and K. Ohki has revealed a great variety of the hard X-ray source structures such as compact single source, large loop-like structures

and multi-component structures. Evolutionary change from one type to
the other and/or mixtures of several kinds of sources in a flare have
also been found. Publications of individual cases are in preparation by
the SXT team. Here, I introduce some of their preliminary results or
results before publications, together with some my own comments (for
example, proposed flare types).

An example of compact single source is shown in Fig.1 (Tsuneta p.c.
-private communication). The source size is very small, about 10"
(7000km) or less and tends to decrease in the post-maximum phase. This
kind of source is characteristic of particular flares marked by high X-
ray intensity of short duration, structureless time profile and very
"soft" hard X-ray spectrum (type A, see Fig.5). Although the flare
showing this characteristic from the initial phase is rather rare,
similar characteristics of the spectrum are often witnessed after the
middle phase of so-called impulsive flares, which are characterized by
spike components in the initial phase (type B). Later phases seem to
correspond to the compact, single (and sometime shrinking) source. From
comparisons with the Hα emissions, the compact source is suggested to be
located at the top of the loop (Tanaka, preliminary results).

A large loop-like structure is reported by Takakura et al. (1982
HS) in a long-duration burst of May 13, 1981 which occurred near the
limb. Superposition of hard X-ray images on the Hα pictures indicates
that X-ray source is located nearly along the tops of the loop arcades
which would connect the Hα two ribbon emissions (Hiei et al. 1982 HS).
This global structure is rather stationary during a long lasting gradual
burst (type C). Existence of the stationary coronal source has been
confirmed in several limb flares, too. Fig.2 shows a case of large limb
flare of X5.5 (Tsuneta et al. 1982 HS). Although the source size appears
to increase slightly during the initial phase, its center of gravity
remains unchanged, at the height of about 15000km above solar photosphere.
The soft X-ray image (Tsuneta, preliminary result) is nearly concentric
to the hard X-ray image and about double in linear size. It may imply
that the hard X-ray source is confined in much smaller portion of the
coronal loops than the soft X-ray source.

Impulsive bursts of short duration (type B) show a variety such as
point-like, arch-like, double, and extended multi-structures (Takakura,
Ohki, p.c.). Some impulsive flares show rapid variations of the source
structure. From the imaging of limb flares it is suggested for some
flares that the sources are low in height, presumably chromospheric
(Ohki, p.c.). An example of double sources which appear cospatial with
the two Hα emissions (Tsuneta, Tanaka, Zirin, and others, preliminary
result) is shown in Fig.3 (top). The double structure is separated by
47000km, and the weaker component soon disappeared. In later phase, as
the intensity variation becomes more gradual the hard X-ray source is
shifted to accord with the top or slightly above the top of a bright Hα
loop which appeared in this phase and connected the two ribbon emissions.
In other limb flare Ohki (p.c.) has reported that the main source stays
at about 10^4 km above the photosphere from the beginning, while a weak
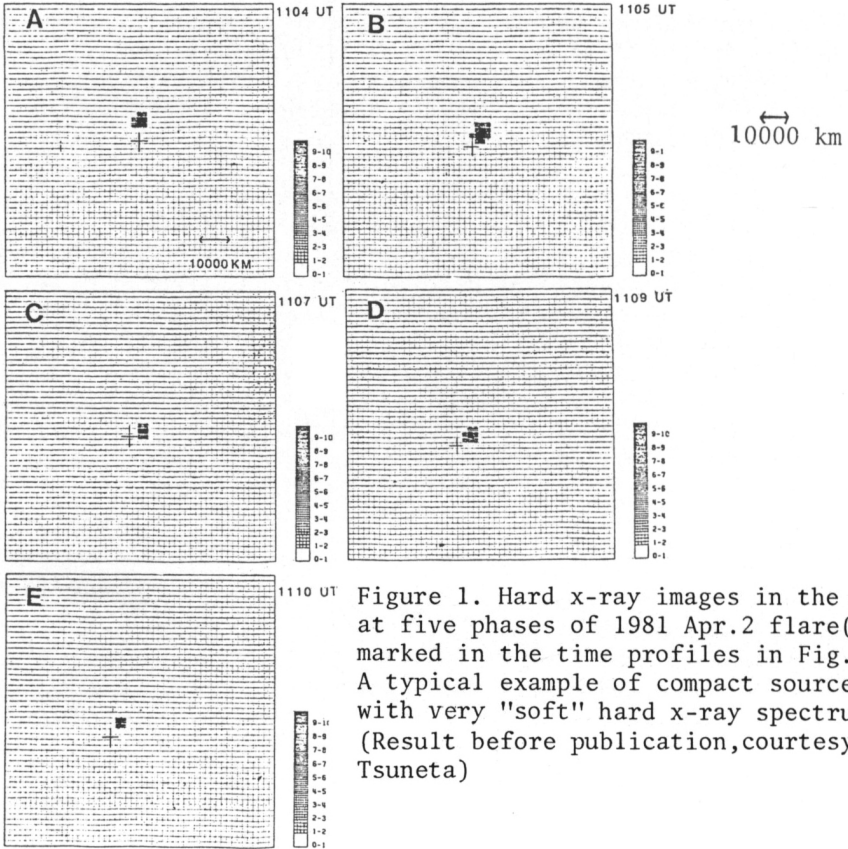
Figure 1. Hard x-ray images in the 17-60 keV
at five phases of 1981 Apr.2 flare(times are
marked in the time profiles in Fig.5).
A typical example of compact source structure
with very "soft" hard x-ray spectrum (type A)
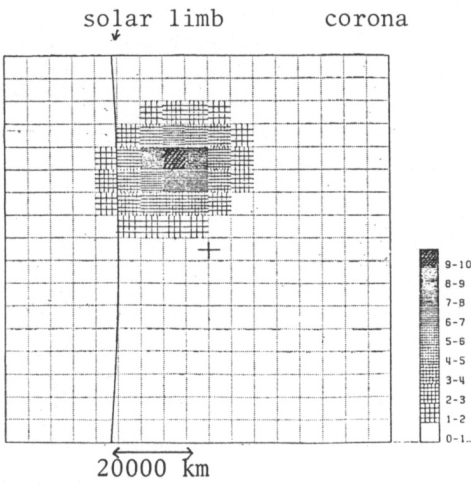(Result before publication,courtesy of Mr.S.
Tsuneta)

Figure 2. Hard x-ray image in the
17-60 keV of 1981 April 27 flare
(limb flare). An example of coronal
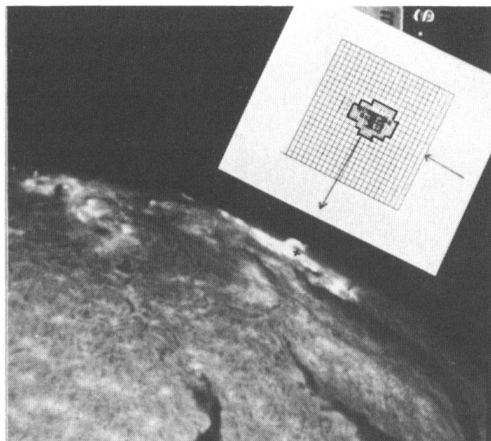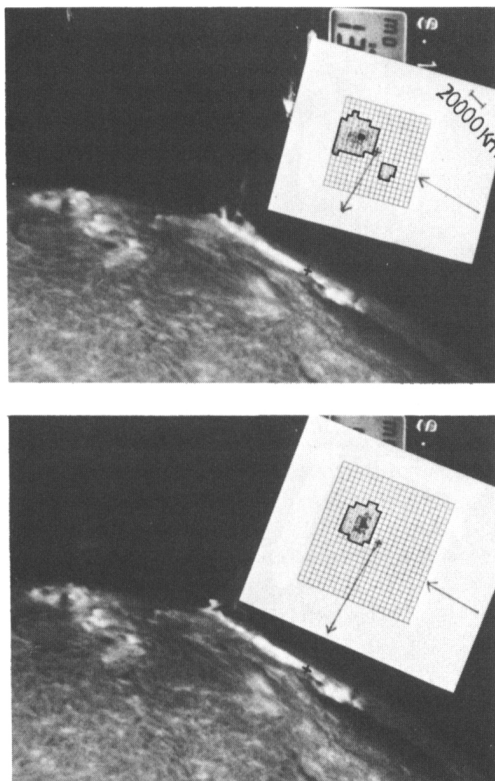source. (Tsuneta et al. 1982HS;
result before publication)

Figure 3. Hard x-ray images in the
17-40 keV and Hα pictures(BBSO) of
1981 July 20 flare.Coordinate centers
of hard x-ray images are marked by
cross in Ha. Example showing change
from double to single sources.
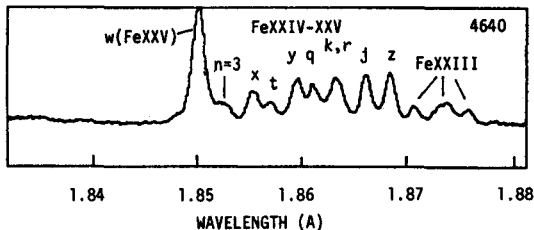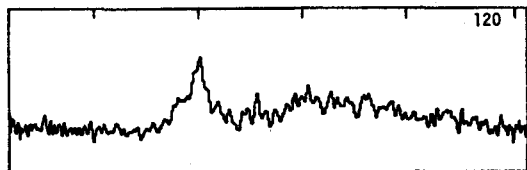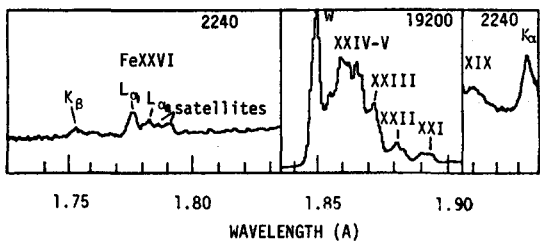(Preliminary result, Tsuneta et al.)

Figure 4. Examples of soft
x-ray iron line spectrum
in 1.73-1.94A (top) and high
dispersion spectra in 1.83-
1.88A(lower two). Note the
line broadening shown in the
middle which is a typical
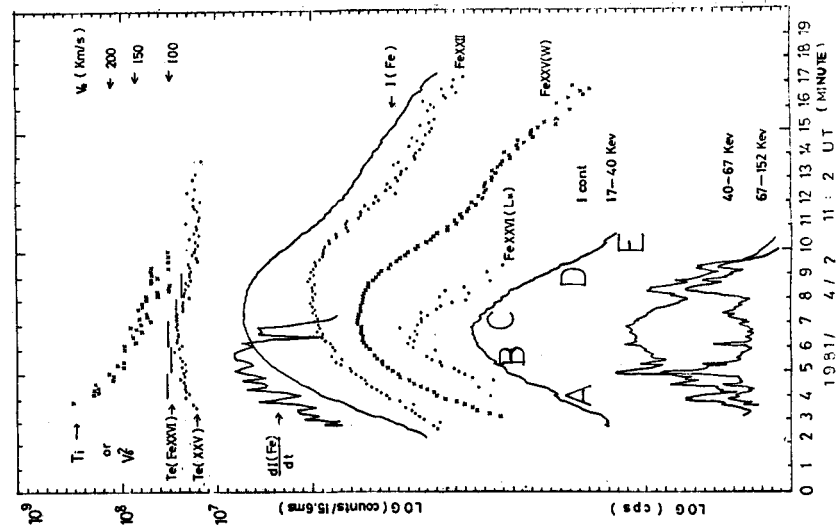spectrum in the flare start.
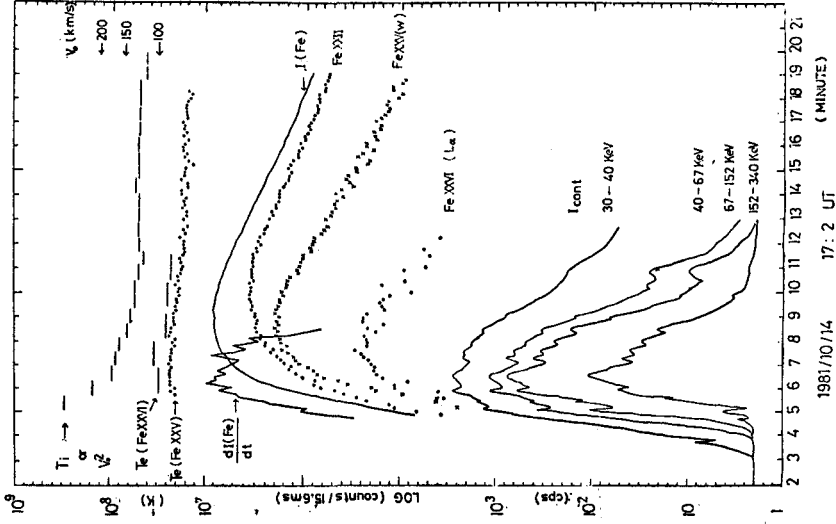
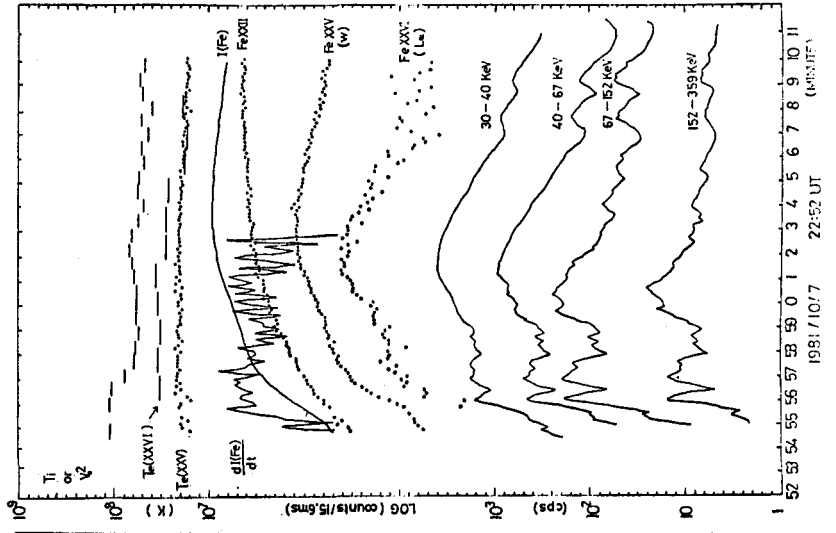Figure 5. (1981 Apr.2-X2.3)

Figure 6. (1981 Oct.14-X3.0)

Figure 7. (1981 Oct.7-X3.6)

Time profiles of various plasma parameters derived from line spectra and intensity time profiles for three types of flares(Fig.5 for type A, Fig.6 for type B and Fig.7 for combined type A and B). From top: ion temperature(turbulence), electron temperature (Fe XXVI), electron temperature(Fe XXV), intensities from Fe XXII, Fe XXV(w), time derivative of total line emissions:I(Fe), total line emissions:I(Fe), intensities from Fe XXII, Fe XXV(w), Fe XXVI(La), continua of 17-40 keV,40-67 keV, 67-152 keV and 152-350 keV.Ordinate in the same log scale.

sub-source, which might be a footpoint of the loop, appears in the
initial phase.

3. RESULTS FROM THE SOFT X-RAY CRYSTAL SPECTROMETERS

The soft X-ray rotating crystal spectrometers (SOX) consist of two
flat SiO_2 crystals and Na(Tl) scintillation counters. The wavelength
scan is made by the satellite spin. Two wavelength regions about 1.72-
1.95A and 1.83-1.89A are scanned in half a spin period (7-10s) with
resolutions of about 2mA and 0.15mA, respectively. About 10 X-class
flares have been analyzed (Tanaka et al. 1982a, b, HS). Fig.4 shows an
example of the spectra. Various plasma parameters have been derived
such as electron temperatures, ionization temperatures, ion temperature
or turbulence, and mass motion. Resolved spetrum of FeXXVI (Lα and
associated satellites) has provided the electron temperature of the
hottest plasma using the line ratio.

Time profiles of obtained plasma parameters are shown, together
with intensity time profiles from the soft to hard X-ray ranges in
Fig.5-Fig.7. Fig.5 refers to an intense flare of "soft" spectrum which
is shown in Fig.1 (type A), Fig.6, a short impulsive flare (type B) and
Fig.7, an extended burst which showed spiky components at the early
phase and gradual component after the middle phase. We have found
remarkable line broadening in the initial few minutes of all flares.
The line widths, if interpreted as thermal broadening, give ion
temperatures exceeding 10^8K, which are much higher than the electron
temperature. It should rather be attributed to the large turbulence
(150-300kms^{-1}). An evidence is given that large broadening exists prior
to the impulsive hard X-ray burst though it is accompanied by a gradual
rise in the hard X-ray. In the very beginning of the line broadening
phase small (10%), blue-shifted components with V=150-400 kms^{-1} are
often seen in the disk flares. In the limb flares the blue- shifted
component cannot be found.

The electron temperature derived from the FeXXV resonance to di-
electronic satellite line ratio (B. Dubau et al. 1982) increases rapidly
to about 20×10^6K in the period of large turbulence. Then, it increases
gradually (upto 25×10^6K) or remains constant and decreases slowly in the
decay phase. Initial temperature increase occurs in a very short time
(10s-1min.) associated with the increase in the emission measure. The
electron temperature derived from the FeXXVI line ratio (Dubau et al.
1981) is equal to $30-40 \times 10^6$K near the maximum, which is much higher than
the electron temperature derived from the FeXXV line ratio but in decay
phase it becomes closer to the latter. Since results obtained conflict
the assumption of uniform temperature, which is adopted in the line
ratio method, we searched for solutions which allow for two temperature
structure using the same set of lines and assuming the ionization
equilibrium. Fig.8 shows an example of temperature and emission measure
diagram thus derived. It shows a clear separation of cooler component
($15-20 \times 10^6$K) from hotter component ($30-50 \times 10^6$K). Evolution of the

LOG EM(CM^{-3})
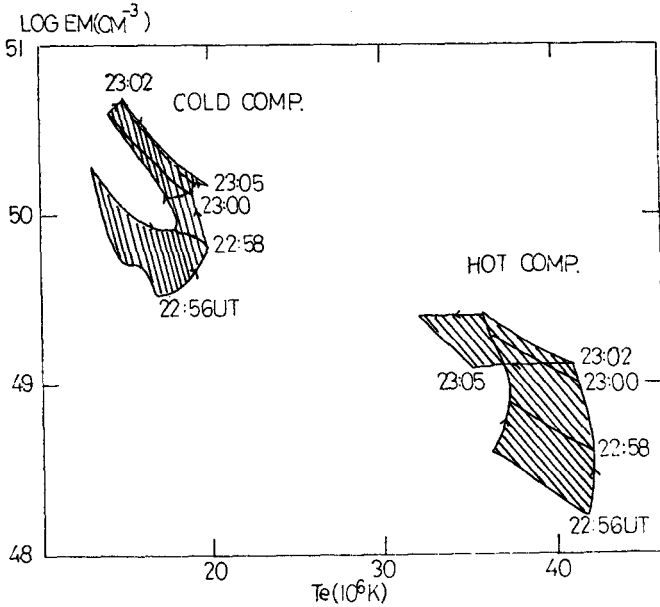
COLD COMP.

23:02

23:05
23:00

22:58

22:56UT

HOT COMP.

23:02
23:05   23:00

22:58

22:56UT

Te(10^6K)

Figure 8. Evolution
of temperatures and
emission measures of
two thermal components
(For flare of Fig.7).

40-340keV

17-40keV

2-5keV
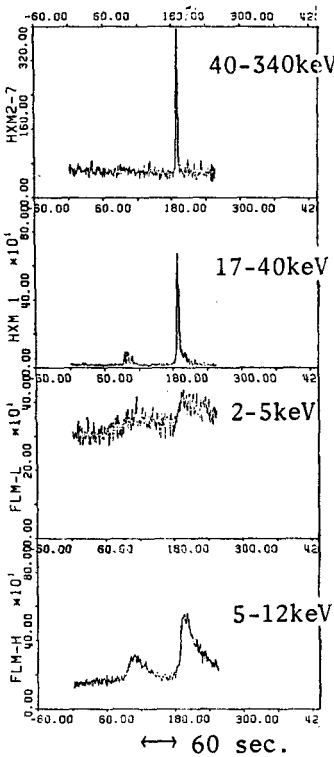
5-12keV

←→ 60 sec.

Figure 9.
Time profiles
of a very
short flare.
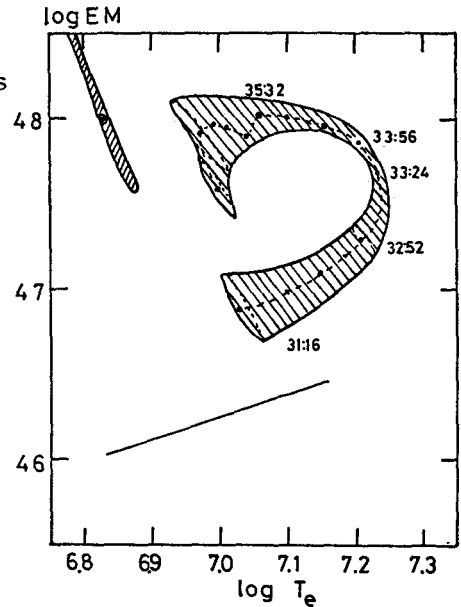
log EM

35:32

33:56
33:24

32:52

31:16

log T_e

Figure 10. Evolution of temperature
and emission measure in a simple
,short flare.(Watanabe et al.1982HS)
A straight line shows a case of
adiabatic compression.

cooler component is reflected in the intensity profiles of lines from
FeXXV or lower ionization, typically the total iron emission : I(Fe),
while the intensity profile of FeXXVI Lα line represents evolution of
the hotter component. Generally the two intensity profiles are different.
Comparisons of the line intensity profiles with those of the hard X-ray
continuum reveal two facts. Firstly, the increase rate of I(Fe) is
propotional to the global intensity variation of the hard X-ray spike
components, especially for the harder range above 40keV. It indicates
close relationship between the productions of the high energy electrons
and the cooler thermal plasma. In particular it has been shown that
thick target electron power input as derived from the hard X-ray spectrum
explains the increase of the thermal energy content for the 10-20 million
degree plasma. The two quantities agree in absolute scale with $Ne=$
10^{11}-10^{12} cm^{-3}, which implies that the electron beams are responsible for
the production of the hot plasma by heating the transition region plasma
of above densities. Presumably the observed blue-shift which is
predominantly vertical to the surface would represent expansion of the
heated plasma into the loop. The low height in the hard X-ray source of
some impulsive flares may suggest thick target hypothesis, too. These
characteristics seem typical for the impulsive phase of flares (type B
phase).

The second fact is that the hard X-ray time profiles, in the low
energy range of 17-40keV, tend to become smooth near the maximum of
flares as well as that their intensity profiles become similar to the
FeXXVI Lα intensity profile. (see Fig.7) This tendency is most pronounced
in type A flare. One can see in Fig.5 the similarity of the two profiles
from the first. In short impulsive burst (type B) the tendency is less
pronounced. For type A flare the emission measures and temperatures of
the hotter thermal component explain the hard X-ray flux in the 17-40keV
range. We may safely conclude that, for this kind of flare, the observed
compact hard X-ray source in this energy range is identical with the
volume of the hotter thermal plasma. Using the hard X-ray source size
and the emission measures of the hotter component we obtain $Ne=10^{11}$-
10^{12} cm^{-3}. The high density is consistent with the observed cooling time
(150s for $\Delta Te=10^{7}$ K) of the hotter component assuming the radiation
cooling. It assures also the ionization equilibrium. It should be
remarked that Hα loop, very bright at the top, appears almost at the
maxima of the smooth hard X-ray component and FeXXVI Lα (BBSO, flare of
Fig.7). It is likely that the highly condensed 30-50 million degree
plasma cools down rapidly at the top of the loop. Above results indicate
that previously unknown plasma component of $Ne= 10^{11}$-$10^{12} cm^{-3}$ and $Te=30$-
50×10^{6} K is formed in the middle phase of impulsive flare or from the
initial phase of some particular flares. This is considered to be
characteristic phenomenon of the type A phase.

4. SIMPLE FLARES

A simple flare, which consists of a single spike of very short
duration, may be considered as elememtary burst, and useful to estimate

elementary flare process. Such burst, as shown in Fig.9, indicates a
hard X-ray burst of 5s FWHM duration and associated soft X-ray burst of
40s FWHM duration. Time integration of the hard X-ray intensity is
precisely proportional to the rising flux of the soft X-ray burst, and
the thick target electron power input above 20keV is shown to be consistent
with the thermal energy content of the soft X-ray emitting plasma with
$Ne=10^{12}cm^{-3}$ (Tanaka et al. 1982 HS). The radiation cooling time of 15
million degree plasma at this density is consistent with the observed
decay time of the soft X-ray burst. These facts suggest production of
the thermal plasma by the electron beam.

    Thermal histories of simple flares have been derived from continuum
spectrum in the range of 2-12keV which is obtained from the scintillation
proportional counter (FLM). This sensitive detector resolves Fe line
and other lines from the continuum (Inoue et al. 1982) which enabled the
analysis of pure continuum. The emission measure-temperature diagram of
a simple flare as derived from the χ^2 minimum condition is shown in
Fig.10 (Watanabe et al. 1982 HS). In small flares like this only cooler
thermal component is produced. It is found that the temperature increases
till the end of the hard X-ray burst, while the emission measure continues
to increase for a minute after that. The temperature, thereafter,
decreases with constant emission measure. If radiation cooling is
assumed, $Ne=10^{11.5}cm^{-3}$ is obtained. The initial increase rates of the
temperature and emission measure happen to satisfy, in this flare, a
relation (shown by a line) which is expected in the adiabatic compression
with the conservation of total mass. However this relation is not
observed in other simple flares, excluding this process as elementary
heating mechanism.

5. DISCUSSIONS - FLARE LOOP MODEL

    Present knowledge of the hard X-ray images is still fragmentary,
and it is still premature to perform self-consistent classification.
However, to promote comparisons with models, I tentatively classify the
reported hard X-ray images into three categories : stationary coronal
source (type C phenomenon), low-chromospheric footprint-source (type B
phase), and compact-coronal-source (type A phase). The coronal source
suggests dissipative model of the hard X-ray burst (Brown et al. 1979;
Smith and Auer 1980) or trapped electron model. Long-enduring electron
trap may be realyzed only for low coronal density. Under the assumption
of thin target emission, Tsuneta et al. (1982HS) derived $Ne=10^9cm^{-3}$ as
the lower limit of the ambient density from the observed hard X-ray
spectrum and source size for the flare shown in Fig.2, and concluded
that the collision time of 20-30keV electron in this density appears to
be too short compared with the burst duration. Therefore, continued
injections of electrons are needed. If the injection occurs in a form
of electron beams, however, the beams will dissipate immediately at this
low density due to the ion-acoustic instability of the return current
associated with the electron beam. (Brown and Melrose 1977).

    In the dissipative model a high temperature (over 10^8K) region will

PHASE 1: $N_e < 6 \times 10^9 \mathrm{cm}^{-3}$ PHASE 2: $6 \times 10^9 < N_e < 10^{11} \mathrm{cm}^{-3}$
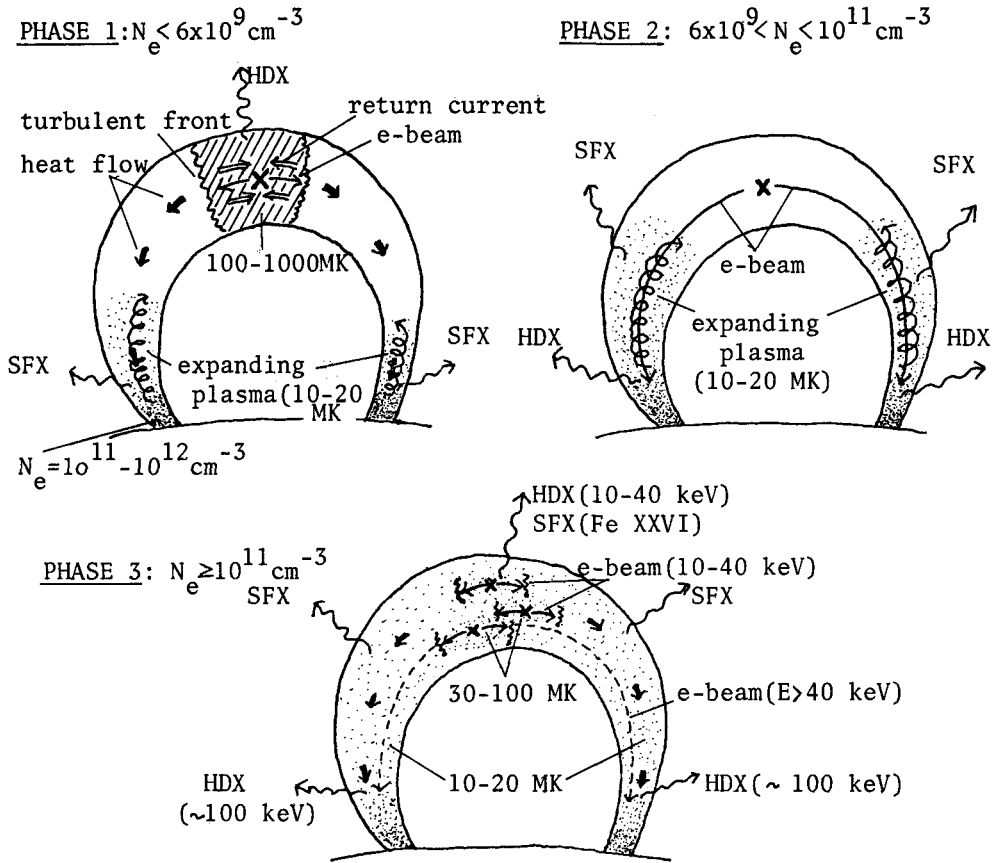

Figure 11. Proposed model of flare loop evolution. As the coronal density increases due to the chromospheric evapolation, hard x-ray source shifts from top of a loop to foot points and again to top. The cross represent energy release site(beam production). HDX:hard x-ray, SFX:soft x-ray MK:million degrees.

be formed at the energy release site, presumably at the loop top. If the dissipation continues, the hot region expands to the whole loop immediately by conduction. The limitation of the conduction due to the anomalous conductivity or due to saturation of conduction does not increase this time scale beyond 10s (Smith and Auer 1980), This situation apparently contradicts the stationary coronal source which is confined in small region. It seems necessary to consider that a heating of short duration (less than 10s) occurs successively in the nearby loops which cannot be resolved by present resolution.

The low (chromospheric) source or double source, on the other hand, suggests thick target emission of hard X-ray at the footpoints of the

loop. Electron beams would be responsible for this case. Electron precipitation and subsequent heating of the dense plasma of low-temperatures appears to be consistent with the soft X-ray results (time profiles of 10-20 million degree plasma and blue-shifts).

   While we cannot discriminate among several energy release modes in the dissipative model, we may note that three types of the burst source can be explained in terms of the electron beam hypothesis as results of evolutionary changes in the ambient density. To illustrate this, we consider continued injection of the electron beams at the top of the loop (Fig.11). When the initial density of the loop is low enough ($Ne < 6 \times 10^9 cm^{-3}$, Tanaka et al. 1982HS), the beam dissipates as noted before and a high temperature (over $10^8 K$) region bounded by the turbulent front will be realyzed for a few seconds (phase 1). Conduction from the hot region will cause ablation of dense transition region, producing 10 million degree plasma. This plasma will expand into the loop and increases slightly the loop density. Then, a condition for the electron beam to stream freely ($Ne > 6.10^9 cm^{-3}$) may be realized, which results in strong beaming down to the footpoints of the loop (phase 2). The thick target hard X-ray emission will occur at the footpoints, together with efficient heating of the transition region or chromophere(type B phase). The heated plasma will expand to fill the loop as the beaming continues, and make the loop density equal to the transition region density or $10^{11}-10^{12} cm^{-3}$. In this phase (phase 3) low energy electrons (10-40keV) in the newly produced beam will be thermalized immediately at the source region due to the collision. Actually the 20keV electron decays within 3000km at $Ne=10^{11} cm^{-3}$. Thus, we have compact, dense hot regions which may consist of plasma of $Te < 10^8 K$ (temperature is expected somewhat low because of low efficiency of heating in the high density) at the top of the loop. This phase may correspond to the type A phase. In actual cases this evolution may occur progressevely in unresolved different loops. Then, we may see coronal source and chromospheric source at the same time. Due to varieties in the initial density of loops, duration of individual heating as well as in the number and size of loops there may occur various types of flare in which particular phase(s) of above sequence would be enhanced. The type C phenomenon may be considered as successive realizations of phase 1 or phase 3 in different unresolvable loops. If the initial density is higher than $10^{10} cm^{-3}$, phase 1 will be skipped and footpoint sources are seen first. Also if the loop size is very small, the expansion time is short and phase 3 may be realyzed from the early phase. This case may explain type A flare.

   Although above scenario may explain qualitatively plasma heating under the unitary electron beam hypothesis, other mechanisms cannot be excluded. Acceleration of protons almost simultaneous with electrons has been suggested from the γ-ray observation from Hinotori (Yoshimori et al. 1982HS), which I have not referred to. Plasma heating as the production of low energy protons might be the other possibility (Enome. p.c.). It seems important to explain the observed line broadening to clarify the heating mechanism.

ACKNOWLEDGEMENTS

REFERENCES

Bely-Dubau,F., Dubau,J., Faucher,P., and Gabriel,A.H. 1982, M.N.R.A.S 198,239.
Brown,J.C. and Melrose,D.B. 1977, Solar Phys. 52, 117
Brown,J.C., Melrose,D.B. and Spicer,D.S. 1979, Ap.J.228, 592.
Dubau,J. et al. 1981, M.N.R.A.S., 195, 705.
Inoue,H., Koyama,K., Mae,T., Matsuoka,M., Ohashi,T., Tanaka,Y. and Waki,I. 1982, Nuclear Instruments and Methods 196, 69.
Smith,D.F. and Auer,L.H. 1980, Ap.J. 238, 1126.

Tanaka,K., Watanabe,T., Nishi,K., and Akita,K. 1982, Ap.J. (letters), 254, L59.
Tanaka,K., Akita,K., Watanabe,T., Miyazaki,H., Kumagai,K., Miyashita,H., Nishi,K. and Moriyama,F. 1982, Annals of Tokyo Astr. Observatory 2nd Series, Vol.18, 237.

DISCUSSION

Kodaira: Do you have microwave coverage for the smooth hard X-ray compact of your observations? Because microwave data usually has the same kind of smooth profile.

Tanaka: Yes. $35GH_z$ shows a slow gradual flare with the same structure as the hard X-ray.

Pallavicini: You apparently explain all of your hard X-ray observations using non-thermal electrons. Can you exclude the possibility of a thermal model for some of these flares?

Tanaka: From the hard X-ray imaging we see that these impulsive bursts are very low in the atmosphere, in the chromosphere. So from that point

of view a non-thermal model is better. However the spectrum itself is exponential which is very strange for this impulsive flare.

Uchida: So the possibility of a thermal model exists.

Simnett: Can I make a comment about the last question? If one considers the ion acceleration derived from the gamma-ray results it is fairly clear that these cannot be explained on a thermal hypothesis. There are certainly many flares where one needs non-thermal acceleration of parti-cles and I think the best proof of this is the gamma-ray observations. Looking purely at the X-ray observations alone it is possible for "non-believers" to "wriggle out" of the non-thermal hypothesis. It is extre-mely difficult to do that with the gamma-ray result.